crystals

MDPI

Communication

Hetero-Trinuclear Co^{II}_2-Dy^{III} Complex with a Octadentate Bis(Salamo)-Like Ligand: Synthesis, Crystal Structure and Luminescence Properties

Yu-Hua Yang, Jing Hao, Xiao-Yan Li, Yang Zhang and Wen-Kui Dong *

School of Chemical and Biological Engineering, Lanzhou Jiaotong University, Lanzhou 730070, China; yangyuhua@mail.lzjtu.cn (Y.-H.Y.); haojingmm@126.com (J.H.); L1401569787@163.com (X.-Y.L.); zhangy8124@163.com (Y.Z.)

* Correspondence: dongwk@126.com; Tel.: +86-931-4938-703

Received: 28 March 2018; Accepted: 16 April 2018; Published: 18 April 2018

Abstract: A hetero-trinuclear Co^{II}_2-Dy^{III} complex, $[Co_2L(DMF)_2Dy(NO_3)_3]\cdot C_2H_5O_2$ was synthesized via the reaction of a multi-naphthol-based bis(Salamo)-like tetraoxime H_4L with $Co(OAc)_2\cdot 4H_2O$ and $Dy(NO_3)_3\cdot 6H_2O$, and fully characterized via elemental analyses, X-ray crystallography, FT-IR and UV-Vis spectra. In addition, luminescence properties of H_4L and its Co^{II}_2-Dy^{III} complex have also been investigated.

Keywords: Salamo-like tetraoxime; Co^{II}_2-Dy^{III} complex; synthesis; crystal structure; luminescence property

1. Introduction

In the past decades, many scientists were working on the study of Salen [1–3] and its analogues [4–9] mainly because their metal complexes can be widely used in obtaining optical [10–13] and magnetic [14] materials, biological fields [15–21], electrochemistry [15–23], ion recognition [24–32], supra-molecular buildings [33,34], catalysis activities [35–38], and so on. In the present study, some appropriate Salen-like compounds (Salamo and its analogues) were selected as a hot topic and there are many reports about the metal complexes including two or more molecules of Salen-like ligands [39–42]. Chemical modifications of substituent or functional groups in the Salen N_2O_2 ligands are effective in exchanging the structures or the main functions of the complexes, such as Salamo N_2O_2 ligand (1,2-Bis(salicylideneaminooxy)ethane), a Salen's analogue, (R–CH=N–O–$(CH)_n$–O–N=CH–R) one of the most versatile ligands [37,43]. Although some Salamo-like complexes have been described, there are poorly reported polynuclear hetero-bimetallic 3d–4f complexes with interesting structures and optical properties [44–48]. Moreover, a key feature of such structures is that trivalent lanthanide ions have higher coordination numbers, larger radius, more flexible coordination geometries and unusual 4f electron construction with larger spin moments and stronger spin-orbit coupling [49], therefore, the lanthanide metal complexes have shown interesting magnetic [50] and distinct luminescent properties [51–54]. In addition, 3d–4f complexes can be widely used in catalysis filed [55–61].

In order to study further the hetero-bimetallic 3d–4f Salamo-like complexes and their optical properties, we have newly designed a novel hetero-trinuclear Co^{II}_2-Dy^{III} complex by the complexation of a multi-naphthol-based symmetric bis(Salamo)-like tetraoxime H_4L with $Co(OAc)_2\cdot 4H_2O$ and $Dy(NO_3)_3\cdot 6H_2O$.

2. Experimental Section

2.1. Materials and Physical Measurements

2-Hydroxy-3-methoxybenzaldehyde, 2-hydroxy-1-naphthaldehyde, methyl trioctyl ammonium chloride, borontribromide and pyridiniumchlorochromate were obtained from Alfa Aesar (New York, NY, USA). The other reagents and solvents were bought from Shanghai Darui Chemical Fine Chemicals Company (Tianjin, China). Solvents and all other chemicals were of analytical grade and used without further purification. Elemental analyses (C, H and N) were carried out with Elemantar GmbH VarioEL V3.00 automatic elemental analysis equipment (Berlin, Germany). Elemental analyses for Co^{II} and Dy^{III} atoms were measured using an IRIS ER/S·WP-1 ICP atomic emission spectrometer (Berlin, Germany). Melting points were measured using an X_4 microscopic melting point apparatus made by Beijing Taike Instrument Limited Company (Beijing, China) and were not corrected. FT-IR spectra were recorded on a VERTEX70 FT-IR spectrophotometer (Bruker, Billerica, MA, USA), with samples prepared as KBr (400–4000 cm^{-1}). UV-Vis absorption spectra in the 200–600 nm range were measured on a Hitachi U-3900H spectrophotometer (Shimadzu, Japan) in mixed solvent (chloroform/methanol = 3:2, v/v). Fluorescent spectra were taken on F-7000 FL spectrophotometer (Shimadzu, Japan). ^{1}H NMR spectra were measured using a German Bruker AVANCE DRX-400 spectrometer (Bruker, AVANCE, Billerica, MA, USA). X-ray single crystal structure was determined via a Bruker Smart Apex CCD diffractometer (Bruker, AVANCE, Billerica, MA, USA).

2.2. Synthesis and Characterization of the Ligand H_4L

H_4L was synthesized according to the early reported method, the ^{1}H NMR (Figure 1), IR and UV-Vis spectra of H_4L are in consistent with the data [62].

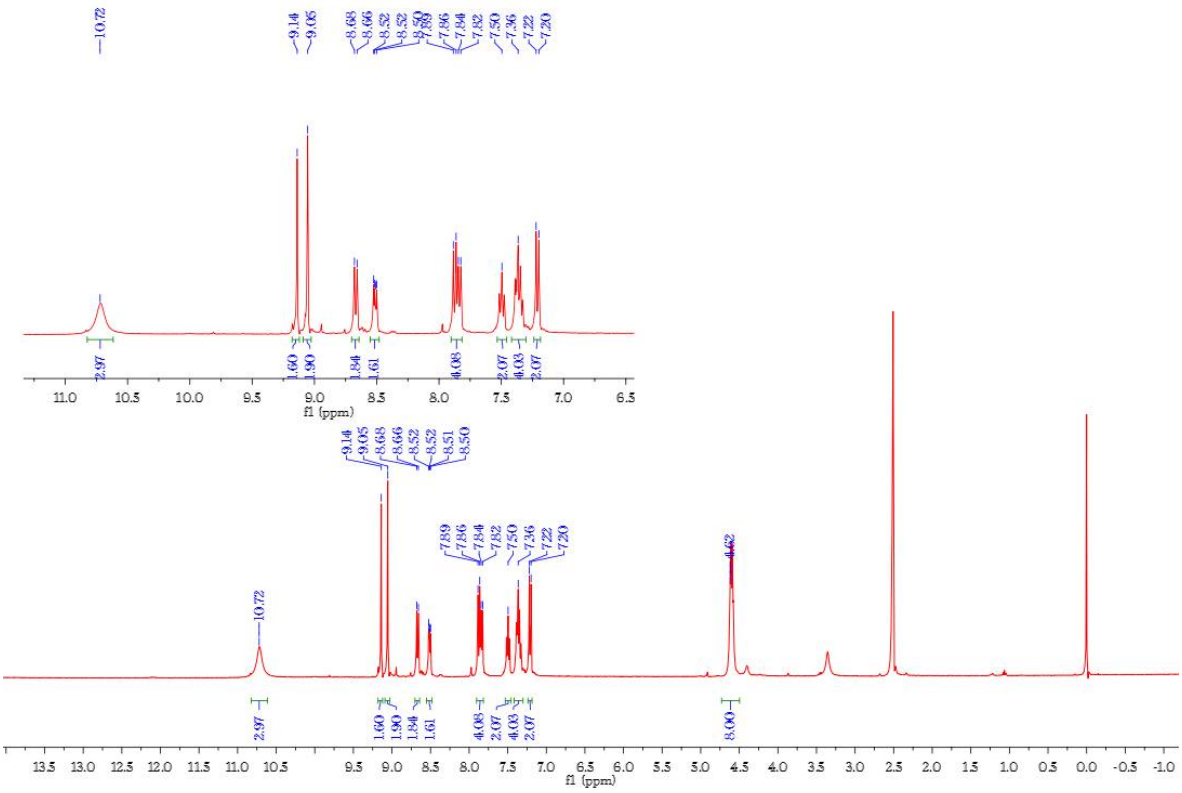

Figure 1. ^{1}H NMR spectrum of the ligand H_4L ($CDCl_3$, 400 MHz).

The step included in the synthetic route to the Co^{II}_2-Dy^{III} complex is shown in Scheme 1.

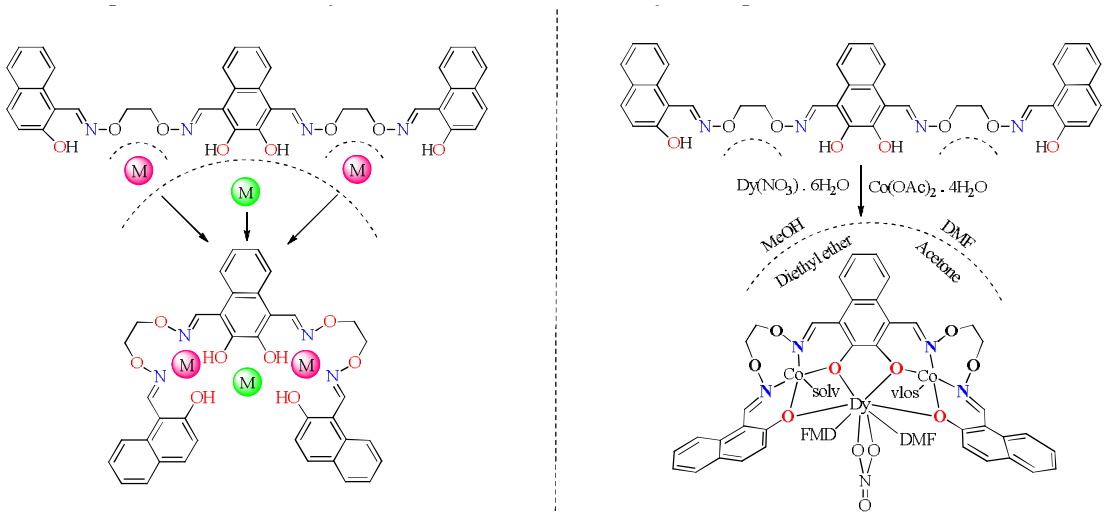

Scheme 1. Synthetic route to the $Co^{II}{}_2$-Dy^{III} complex.

2.3. Synthesis of the $Co^{II}{}_2$-Dy^{III} Complex

A solution of $Co(OAc)_2{\cdot}4H_2O$ (14.94 mg, 0.06 mmol) in methanol (2 mL) and $Dy(NO_3)_3{\cdot}6H_2O$ (9.13 mg, 0.02 mmol) in methanol (1 mL) were added to a solution of H_4L (13.44 mg, 0.02 mmol) in acetone/DMF (1:1, 1 mL) with constant stirring. After about 30 min later, the color of the mixture turned to brown immediately, the brown mixture obtained was filtered and the filtrate was kept undisturbed at diethyl ether. One week later, clear dark brown block-like crystals suitable for X-ray diffraction were formed and carefully collected by filtration, washed with 2:1 (*v*/*v*) acetone:hexane, and dried at room temperature. Yield: 46%. IR (KBr; cm^{-1}): 1594 [*v*(C=N), s], 1249 [*v*(Ar–O), s]. Anal. Calcd. for $C_{52}H_{62}Co_2DyN_9O_{21}$ (%): C, 43.69; H, 4.37; N, 8.82; Co., 8.25; Dy, 11.37. Found: C, 43.91; H, 4.56; N, 8.56; Co., 8.03; Dy, 11.21.

2.4. X-ray Structure Determination of the $Co^{II}{}_2$-Dy^{III} Complex

The single crystal of the $Co^{II}{}_2$-Dy^{III} complex with approximate dimensions of 0.26 × 0.24 × 0.23 mm, was placed on Bruker Smart 1000 CCD area detector. The crystal diffraction data were collected using a graphite monochromated Mo *K*α radiation (λ = 0.071073 nm) at 293(2) K. The structure was solved the using the program SHELXS-2015 and Fourier difference techniques, and refined by full-matrix least-squares method on F^2 using SHELXL-2015 [63]. Hydrogen atoms were fixed at calculated positions, and their positions were refined by a riding model. Details of the data collection and refinements are presented in Table 1.

Table 1. Crystal data and structure refinements for the $Co^{II}{}_2$-Dy^{III} complex.

	$[Co_2L(DMF)_2Dy(NO_3)_3]{\cdot}C_2H_5O_2$
Formula	$C_{52}H_{62}Co_2DyN_9O_{21}$
Formula weight	1429.46
Temperature (K)	293(2)
Wavelength (Å)	0.71073
Crystal system	monoclinic
Space group	P_12_1/m_1
a (Å)	9.2838(4)
b (Å)	24.9653(11)
c (Å)	12.7982(6)
β (°)	97.059(4)°
V (Å^3)	2943.8(2)
Z	2
D_{calc} ($g{\cdot}cm^{-3}$)	1.613

Table 1. *Cont.*

	$[Co_2L(DMF)_2Dy(NO_3)_3]\cdot C_2H_5O_2$
μ (mm^{-1})	1.897
Formula	$C_{52}H_{62}Co_2DyN_9O_{21}$
F (000)	1450
Crystal size (mm)	0.26 × 0.24 × 0.23
θ Range (°)	3.310–26.017
Index ranges	$-11 \leq h \leq 10$ $-30 \leq k \leq 25$ $-15 \leq l \leq 11$
Reflections collected	11,948
Independent reflections	5933
R_{int}	0.0456
Completeness to θ	99.7% (θ = 26.32)
Data/restraints/parameters	5933/3/422
GOF	1.028
Final R_1, wR_2 indices [I > 2σ(I)]	0.0426/0.0758
Final R_1, wR_2 indices (all data)	0.0590/0.0854
Largest differences peak and hole (e $Å^{-3}$)	0.840/−1.044

Supplementary crystallographic data for this paper have been deposited at Cambridge Crystallographic Data Centre (1817410) and can be obtained free of charge via www.ccdc.cam.ac.uk/conts/retrieving.html.

3. Results and Discussion

3.1. IR Spectra of H_4L and Its Corresponding $Co^{II}{}_2$-Dy^{III} Complex

The FT-IR spectra of H_4L and its corresponding $Co^{II}{}_2$-Dy^{III} complex exhibited various bands in the range of 400–4000 cm^{-1}. As depicted in Figure 2, H_4L showed a typical C=N stretching band at ca. 1613 cm^{-1} [64,65], while the C=N stretching band of the $Co^{II}{}_2$-Dy^{III} complex was observed at ca. 1594 cm^{-1}. The shift to lower frequency by ca. 19 cm^{-1} upon complexation shows a decrease in the C=N bond order due to the coordinative bonds of the metal atom with the oxime nitrogen lone pair [66]. The Ar–O typical stretching band of H_4L appeared as a strong band at ca. 1258 cm^{-1}, but was observed at ca. 1249 cm^{-1} for the $Co^{II}{}_2$-Dy^{III} complex and shift to lower frequency by ca. 9 cm^{-1} in the $Co^{II}{}_2$-Dy^{III} complex, exhibiting that the Co-O_{Ar} and Dy-O_{Ar} bonds were formed between phenolic oxygen atoms and the metal atoms [67–69]. Besides, the coordinated nitrate groups appeared at ca. 1300 cm^{-1} for the $Co^{II}{}_2$-Dy^{III} complex [23]. Furthermore, the O–H stretching bands appeared at ca. 3419 cm^{-1} in H_4L [70], and disappeared in the $Co^{II}{}_2$-Dy^{III} complex.

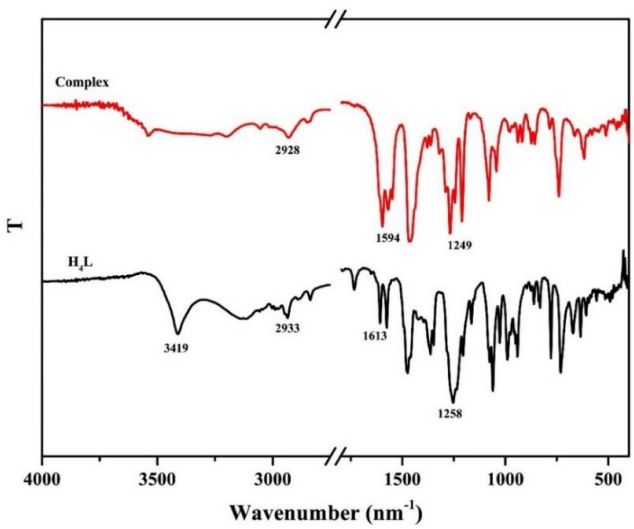

Figure 2. IR spectra of H_4L and its corresponding $Co^{II}{}_2$-Dy^{III} complex.

3.2. UV-Vis Absorption Spectra of H_4L and Its Corresponding $Co^{II}{}_2$-Dy^{III} Complex

UV-Vis spectra of H_4L and its corresponding $Co^{II}{}_2$-Dy^{III} complex in mixed solutions (chloroform/methanol = 3:2, v/v) at 298 K are shown in Figure 3. The spectrum of H_4L was almost consistent with the reported earlier [62]. In the UV–Vis titration experiments of $Co^{II}{}_2$-Dy^{III} complex, the color of the solution of Co^{II} complex in mixed solutions (chloroform/methanol = 3:2, v/v) changed inconspicuously when the solution of Dy^{III} ion was added. However, the $Co^{II}{}_2$-Dy^{III} complex displayed three absorption bands at ca. 317, 374, and 419 nm, which shown red-shifted and indicate the coordination of H_4L with metal ions [70–74]. In addition, the molar absorption coefficient at 374 and 322 nm for the $Co^{II}{}_2$-Dy^{III} complex in mixed solutions (chloroform/methanol = 3:2, v/v) are 29,200 and 18,900 $M^{-1}\cdot cm^{-1}$, respectively. As in the case for the $Co^{II}{}_2$-Dy^{III} complex, although H_4L has two Salamo chelate units, the titration curves clearly indicated that the stoichiometry between Dy^{III} ion and $[LCo_3]^{2+}$ was 1:1, and the isosbestic points (319, 351 and 401 nm) were observed.

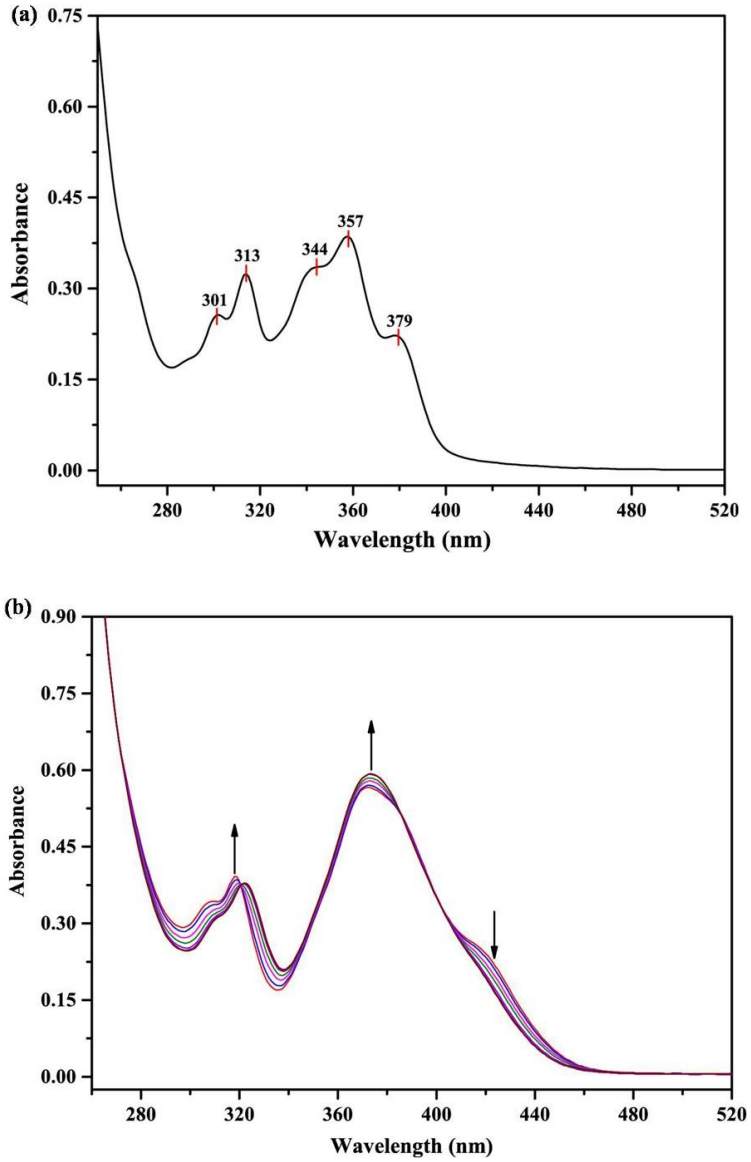

Figure 3. (**a**) UV-Vis absorption spectra of H_4L (c = 1 × 10^{-5} M). (**b**) Absorption spectra of the $Co^{II}{}_2$-Dy^{III} complex in the presence of different concentrations of Dy^{III} ion in mixed solutions (chloroform/methanol = 3:2, v/v) at 298 K.

3.3. Description of Crystal Structure of the $Co^{II}{}_2$-Dy^{III} Complex

The crystal structure of the $Co^{II}{}_2$-Dy^{III} complex and the coordination environment of Co^{II} and Dy^{III} atoms are shown in Figure 4. Selected bond lengths and angles are summed in Table 2.

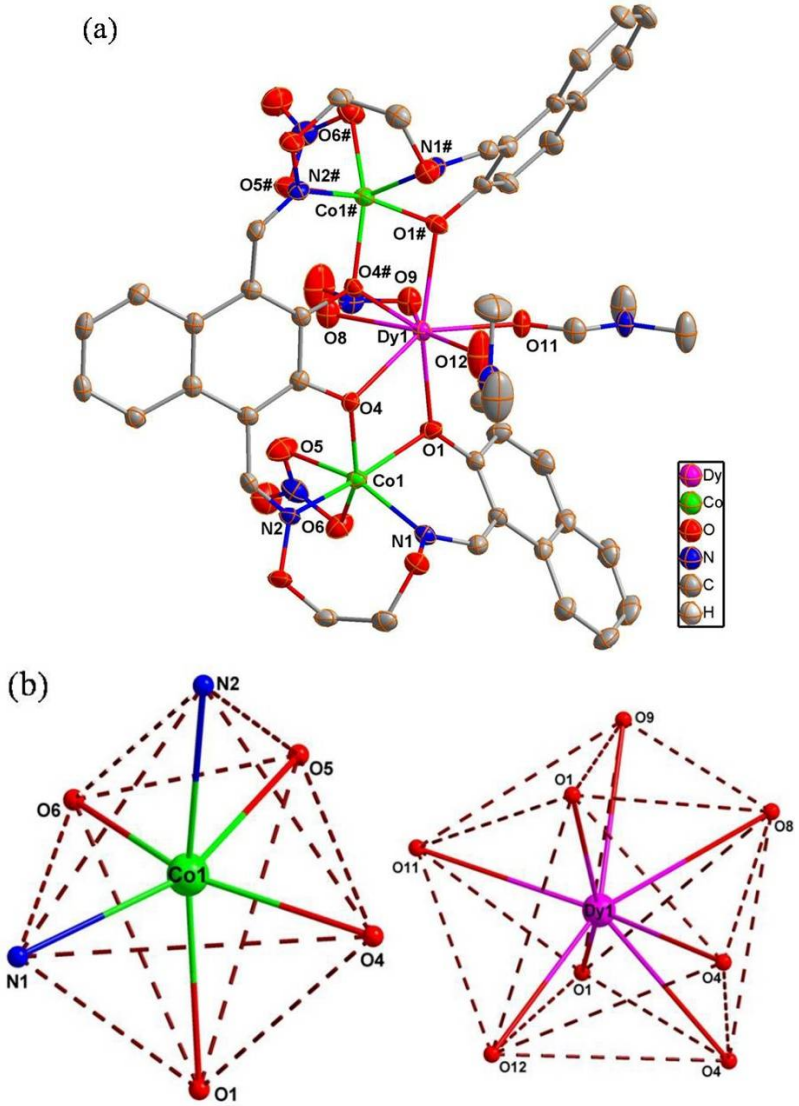

Figure 4. (**a**) Molecular structure of the $Co^{II}{}_2$-Dy^{III} complex. (**b**) The coordination polyhedrons for Co^{II} and Dy^{III} atoms.

X-ray structure analysis showed the $Co^{II}{}_2$-Dy^{III} complex crystallizes in the monoclinic system, space group P_12_1/m_1 with cell dimensions a = 9.2838(4), b = 24.9653(11), c = 12.7982(6), and Z = 2. It is composed of two Co^{II} atoms, one Dy^{III} atom, one deprotonated $(L)^{4-}$ unit, three coordinated nitrate groups, and two coordinated *N*,*N*-dimethylformamide molecules resulting in a hetero-trinuclear $Co^{II}{}_2$-Dy^{III} complex. In the $Co^{II}{}_2$-Dy^{III} complex, two terminal Co^{II} atoms are both six-coordinated with geometries of slightly distorted octahedron. The inner N_2O_2 coordination spheres of Salamo moieties were occupied by two terminal Co1 and Co1$^{\#}$ atoms, meanwhile, two bidentate nitrate groups coordinated two terminal Co^{II} atoms. Dy^{III} is sited in the O_4 cavity that includes four phenoxy oxygen atoms (O1, O4, and O1$^{\#}$, O4$^{\#}$). Besides, the two coordinated DMF molecules provide two oxygen atoms (O11 and O12) and the bidentate nitrate groups provide remaining two oxygen atoms (O8 and O6), so Dy^{III} is eight–coordinated and possesses a distorted square antiprism geometry. Compared with

our previously reported Co^{II} complex [62], Co^{II} atoms are in N_2O_2 coordination environments, and particularly the Co^{II} atoms are chelated further with one bidentate nitrate group. The distance between the two terminal metal atoms Co1-Co1$^{\#}$ is 6.322(3), in the previously reported Co^{II} complex the distance of Co1-Co3 is 6.304(3). The distance of Co1-Co1$^{\#}$ is longer than previously reported, because the larger radius Dy^{III} atom replaced the central Co^{II} atom. The angles of O2-N1-C11, O1-C1-C2 and C10-C11-N1 are 113.7(3), 116.8(4) and 123.3(4), respectively, indicating that the ligand H_4L is more flexible.

Table 2. Selected bond lengths (Å) and angles (°) for the $Co^{II}{}_2$-Dy^{III} complex.

Bond	Lengths	Bond	Lengths	Bond	Lengths
Dy1–O1$^{\#1}$	2.339(3)	Dy1–O9	2.480(4)	Co1–O1	2.104(3)
Dy1–O1	2.339(3)	Dy1–O11	2.316(3)	Co1–O4	1.983(3)
Dy1–O4$^{\#1}$	2.383(2)	Dy1–O12	2.275(5)	Co1–O5	2.210(3)
Dy1–O4	2.383(2)	Dy1–O12$^{\#1}$	2.275(5)	Co1–O6	2.159(3)
Dy1–O8	2.400(4)	Dy1–N4	2.861(5)	Co1–N1	2.034(3)
Bond	**Angles**	**Bond**	**Angles**	**Bond**	**Angles**
O1$^{\#1}$–Dy1–O1	158.66(13)	O9–Dy1–N4	26.13(13)	O12–Dy1–O11	76.66(17)
O1$^{\#1}$–Dy1–O4	132.84(9)	O11–Dy1–O1$^{\#1}$	80.97(6)	O12$^{\#1}$–Dy1–O11	76.66(17)
O1–Dy1–O4	68.05(9)	O11–Dy1–O1	80.97(6)	O12$^{\#1}$–Dy1–O12	18.2(5)
O1–Dy1–O4$^{\#1}$	132.84(9)	O11–Dy1–O4	142.30(8)	O12–Dy1–N4	170.7(2)
O1$^{\#1}$–Dy1–O4$^{\#1}$	68.05(9)	O11–Dy1–O4$^{\#1}$	142.30(8)	O12$^{\#1}$–Dy1–N4	170.7(2)
O1–Dy1–O8	91.00(7)	O11–Dy1–O8	127.46(15)	O1–Co1–O5	100.03(12)
O1$^{\#1}$–Dy1–O8	91.00(7)	O11–Dy1–O9	75.60(14)	O1–Co1–O6	91.67(12)
O1$^{\#1}$–Dy1–O9	82.29(7)	O11–Dy1–N4	101.74(15)	O4–Co1–O1	80.49(11)
O1–Dy1–O9	82.29(7)	O12–Dy1–O1	102.3(2)	O4–Co1–O5	91.68(12)
O1–Dy1–N4	86.31(7)	O12$^{\#1}$–Dy1–O1$^{\#1}$	102.3(2)	O4–Co1–O6	147.62(12)
O1$^{\#1}$–Dy1–N4	86.31(7)	O12–Dy1–O1$^{\#1}$	84.4(2)	O4–Co1–N1	111.71(12)
O4$^{\#1}$–Dy1–O4	64.84(12)	O12$^{\#1}$–Dy1–O1	84.4(2)	O4–Co1–N2	87.13(12)
O4$^{\#1}$–Dy1–O8	75.65(11)	O12–Dy1–O4$^{\#1}$	79.37(18)	O6–Co1–O5	58.58(12)
O4–Dy1–O8	75.65(11)	O12$^{\#1}$–Dy1–O4	79.37(18)	N1–Co1–O1	82.90(12)
O4–Dy1–O9	118.79(10)	O12$^{\#1}$–Dy1–O4$^{\#1}$	89.13(18)	N1–Co1–O5	156.54(14)
O4$^{\#1}$–Dy1–O9	118.79(10)	O12–Dy1–O4	89.13(18)	N1–Co1–O6	98.23(13)
O4$^{\#1}$–Dy1–N4	97.30(12)	O12$^{\#1}$–Dy1–O8	154.48(18)	N1–Co1–N2	94.30(13)
O4–Dy1–N4	97.30(12)	O12–Dy1–O8	154.48(18)	N2–Co1–O1	165.20(12)
O8–Dy1–O9	51.86(14)	O12$^{\#1}$–Dy1–O9	150.76(17)	N2–Co1–O5	88.34(13)
O8–Dy1–N4	25.73(14)	O12–Dy1–O9	150.76(17)	N2–Co1–O6	103.12(13)

Symmetry transformations used to generate equivalent atoms: $^{\#1}$ x, 1/2-y, z.

3.4. Supramolecular Interactions of the $Co^{II}{}_2$-Dy^{III} Complex

Notably, there are various intra- and inter-molecular hydrogen bond interactions in the crystal structure of the $Co^{II}{}_2$-Dy^{III} complex. The hydrogen bond parameters are summed in Table 3. As shown in Figure 5.

There are three pairs of intra-molecular hydrogen bond interactions (C13–H13B···O6, C20–H20···O12 and C22–H22B···O11) [75,76]. Besides, the structure of the $Co^{II}{}_2$-Dy^{III} complex is stabilized by inter-molecular O–H···O, C–H···O and C–H···π hydrogen bond interactions. As a result, the $Co^{II}{}_2$-Dy^{III} complex possesses a self-assembling infinite 2D and 3D supra-molecular structure [77] via the inter-molecular hydrogen bonds, respectively (Figure 6). The 3D supra-molecular structure of the $Co^{II}{}_2$-Dy^{III} complex includes two parts. The former is linked via inter-molecular O–H···O and C–H···O hydrogen bond interactions. The latter is composed of the C–H···π interactions. The inter-molecular hydrogen bonding of the $Co^{II}{}_2$-Dy^{III} complex makes its structure variable and stable. There is no π···π interactions in the $Co^{II}{}_2$-Dy^{III} complex because the distance between ring centroids was 5.953(2) which beyond the specified range.

Table 3. Hydrogen bonding interactions (Å, °) for the Co^{II}_2-Dy^{III} complex [a].

D–H···A	H···A	D···A	D–H···A	Symmetry Codes
C13–H13B··· O6	2.58	3.497(6)	158	
C20–H20··· O12	2.53	3.041(8)	115	
O8–H8 ···O7	2.57	3.378(6)	145	1-*x*, 1-*y*, -*z*
O12–H12A ···O7	2.51	3.476(6)	174	1-*x*, 1-*y*, -*z*
C20–H20··· O10	2.54	3.403(7)	154	-1+*x*, *y*, *z*
C21–H21A··· O10	2.46	3.358(9)	155	-1+*x*, *y*, *z*
C21–H21C··· O13	2.46	3.421(6)	176	*x*, 1/2-*y*, *z*
C13–H13A··· Cg1	2.79		140	1-*x*, 1-*y*, -*z*
C27–H27A··· Cg2	2.70		167	*x*, *y*, *z*
C24–H24C··· Cg3	2.72		122	-1+*x*, 1/2-*y*, *z*
C22–H22B··· Cg4	2.97		107	*x*, 1/2-*y*, 1+*z*

[a] Cg1, Cg2, Cg3 and Cg4 for the Co^{II}_2-Dy^{III} complex are the centroids of C1–C4, C9, C10; C4–C9; C15, C16, C16#, 15#, C17#, C17and C17–C19, 19#–C17# atoms, respectively.

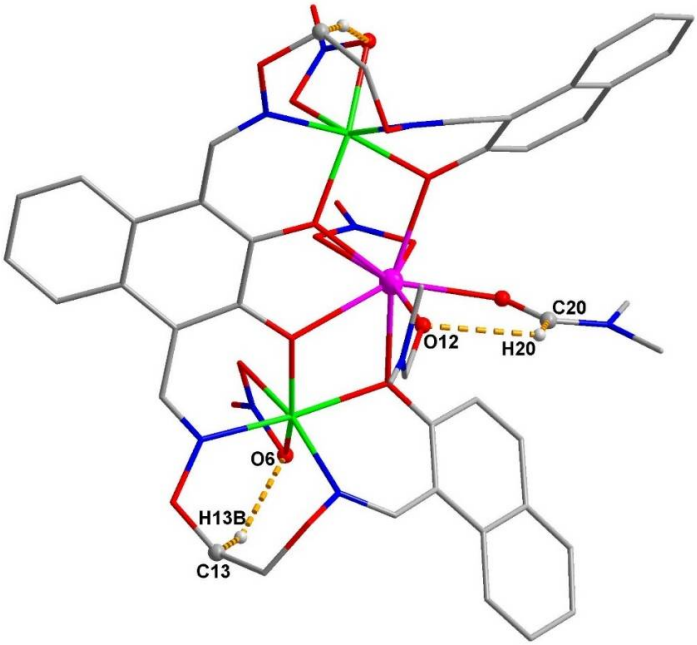

Figure 5. Intramolecular hydrogen bonding interactions of the Co^{II}_2-Dy^{III} complex.

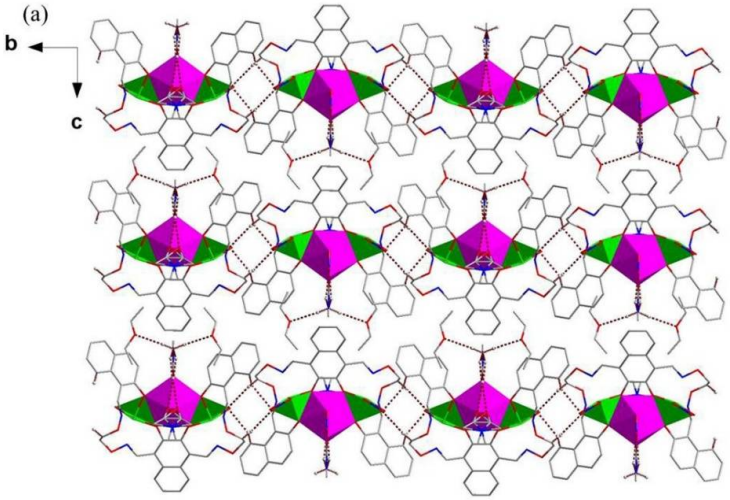

Figure 6. *Cont.*

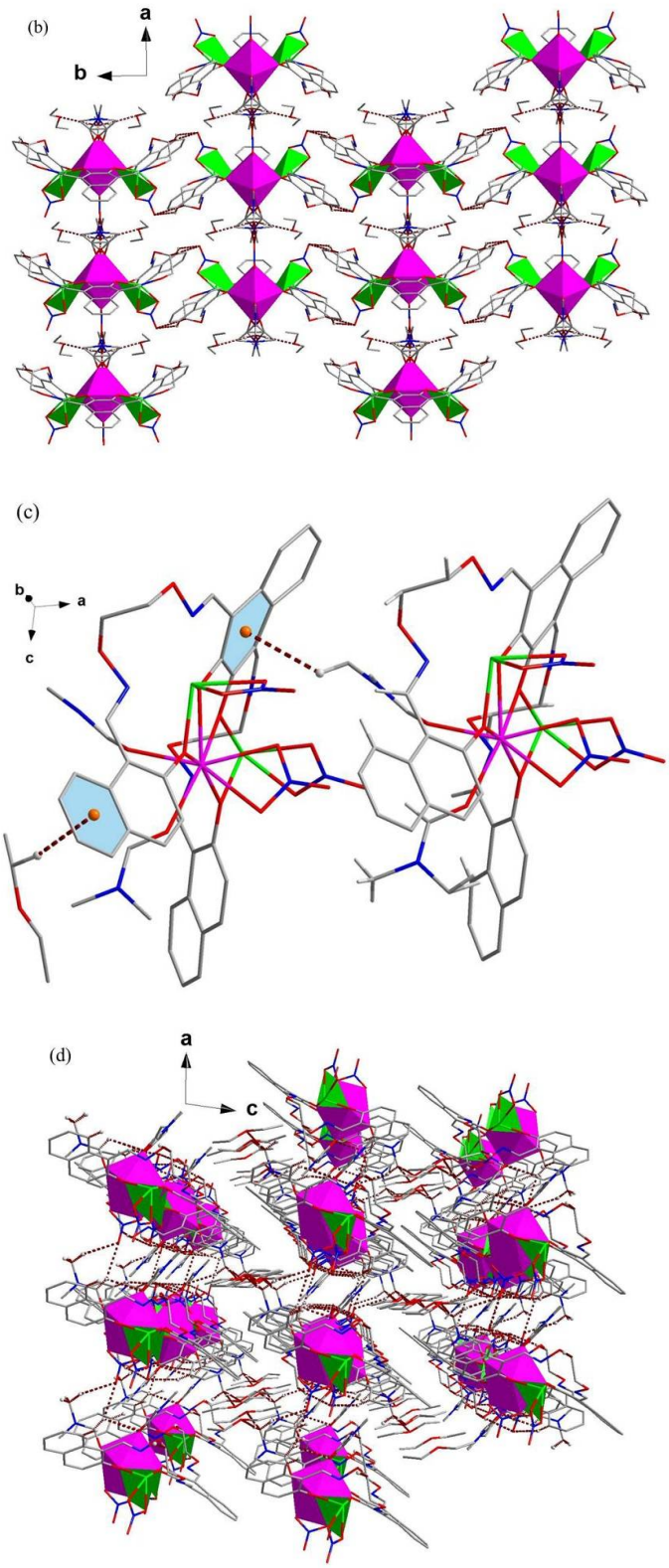

Figure 6. Part of the infinite 2D supra-molecular structure along *a* axis (**a**); *c* axis (**b**); C–H···π (**c**) and 3D (**d**) supra-molecular structure of the Co^{II}_2-Dy^{III} complex with intermolecular hydrogen bondings (hydrogen atoms, except those forming hydrogen bonds, are omitted for clarity).

3.5. Fluorescence Properties of the $Co^{II}{}_2$-Dy^{III} Complex

The emission spectra of H_4L and its $Co^{II}{}_2$-Dy^{III} complex in dilute DMF solution at room temperature are depicted in Figure 7. H_4L showed an intense photoluminescence with maximum emission at ca. 431 nm when excited at ca. 372 nm, which can be attributed to intra-ligand π–π* transitions. Meanwhile, compared with H_4L, the $Co^{II}{}_2$-Dy^{III} complex showed slightly weaker fluorescence intensity with maximum emissions at ca. 421 nm upon excitation at ca. 372 nm, which are attributed to the intra-ligand π–π* transition and exhibiting that the fluorescent behaviour has been affected by the Co^{II} atoms [78]. The bathochromic indicates the hetero-trinuclear structure led to a larger conjugate system [72].

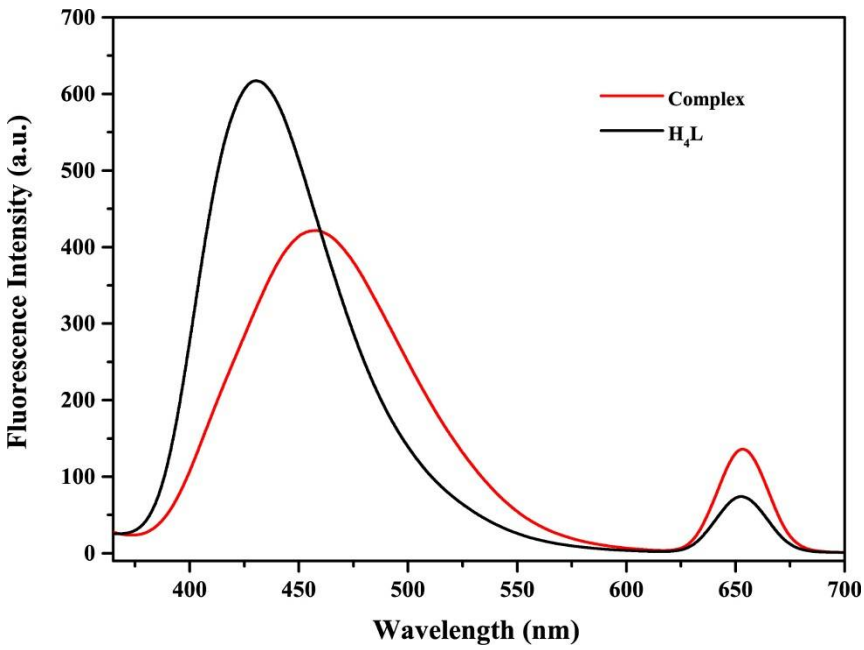

Figure 7. Fluorescence spectra of H_4L and its $Co^{II}{}_2$-Dy^{III} complex ($c = 1 \times 10^{-5}$ M) upon excitation at ca. 372 nm in mixed solutions (chloroform/methanol = 3:2, v/v) at 298 K.

4. Conclusions

We have newly designed a novel hetero-trinuclear $Co^{II}{}_2$-Dy^{III} complex with a multi-naphthol-based bis(Salamo)-like tetraoxime H_4L. The $Co^{II}{}_2$-Dy^{III} complex has been characterized via X-ray diffraction and physicochemical methods. In the $Co^{II}{}_2$-Dy^{III} complex, two terminal Co^{II} atoms, sited in the N_2O_2 cavities of the Salamo units, bear distorted octahedral geometries, and the central O_4 coordination environment was occupied by the Dy^{III} atom bearing a distorted square antiprism. Significantly, the $Co^{II}{}_2$-Dy^{III} complex possesses a self-assembling infinite 2D and 3D supra-molecular structure through the inter-molecular hydrogen bondings which make its structure variable and stable. Compared with H_4L, the $Co^{II}{}_2$-Dy^{III} complex exhibited slightly lower fluorescence intensity, and shifted to higher wavelength, indicating the hetero-trinuclear structure led to a larger conjugate system.

Supplementary Materials: The crystallographic data is available online at http://www.mdpi.com/2073-4352/8/4/174/s1.

Acknowledgments: This work was supported by the National Natural Science Foundation of China (21761018) and the Program for Excellent Team of Scientific Research in Lanzhou Jiaotong University (201706), both of which are gratefully acknowledged.

Author Contributions: Yu-Hua Yang and Jing Hao performed most of the experiments. Xiao-Yan Li and Yang Zhang contributed to the writing of the manuscript. Wen-Kui Dong designed the project. All authors reviewed the manuscript.

Conflicts of Interest: The authors declare no competing financial interests.

References

1. Song, X.Q.; Peng, Y.J.; Chen, G.Q.; Wang, X.R.; Liu, P.P.; Xu, W.Y. Substituted group-directed assembly of Zn(II) coordination complexes based on two new structural related pyrazolone based Salen ligands: Syntheses, structures and fluorescence properties. *Inorg. Chim. Acta* **2015**, *427*, 13–21. [CrossRef]
2. Song, X.Q.; Xing, D.Y.; Lei, Y.K.; Zhao, M.M.; Cheng, G.Q. Lanthanide coordination polymers constructed by a new semirigid bridging salicylamide ligand: Synthesis, supramolecular structure and luminescence properties. *Inorg. Chim. Acta* **2013**, *404*, 113–122. [CrossRef]
3. Song, X.Q.; Liu, P.P.; Xiao, Z.R.; Li, X.; Liu, Y.A. Four polynuclear complexes based on a versatile salicylamide salen-like ligand: Synthesis, structural variations and magnetic properties. *Inorg. Chim. Acta* **2015**, *438*, 232–244. [CrossRef]
4. Sun, Y.X.; Gao, X.H. Synthesis, characterization, and crystal structure of a new Cu^{II} complex with salen-type ligand. *Synth. React. Inorg. Met.-Org. Nano-Met. Chem.* **2011**, *41*, 973–978. [CrossRef]
5. Dong, W.K.; Li, X.L.; Wang, L.; Zhang, Y.; Ding, Y.J. A new application of Salamo-type bisoximes: As a relay-sensor for Zn^{2+}/Cu^{2+} and its novel complexes for successive sensing of H^+/OH^-. *Sens. Actuators B* **2016**, *229*, 370–378. [CrossRef]
6. Sun, Y.X.; Xu, L.; Zhao, T.H.; Liu, S.H.; Liu, G.H.; Dong, X.T. Synthesis and crystal structure of a 3D supramolecular copper(II) complex with 1-(3-{[(E)-3-bromo-5-chloro-2-hydroxybenzylidene]amino}phenyl) ethanone oxime. *Synth. React. Inorg. Met.-Org. Nano-Met. Chem.* **2013**, *43*, 509–513. [CrossRef]
7. Dong, W.K.; Akogun, S.F.; Zhang, Y.; Sun, Y.X.; Dong, X.Y. A reversible "turn-on" fluorescent sensor for selective detection of Zn^{2+}. *Sens. Actuators B* **2017**, *238*, 723–734. [CrossRef]
8. Wang, B.J.; Dong, W.K.; Zhang, Y.; Akogun, S.F. A novel relay-sensor for highly sensitive and selective detection of Zn^{2+}/Pic^- and fluorescence on/off switch response of H^+/OH^-. *Sens. Actuators B* **2017**, *247*, 254–264. [CrossRef]
9. Wang, F.; Gao, L.; Zhao, Q.; Zhang, Y.; Dong, W.K.; Ding, Y.J. A highly selective fluorescent chemosensor for CN^- based on a novel bis(salamo)-type tetraoxime ligand. *Spectrochim. Acta A* **2018**, *190*, 111–115. [CrossRef] [PubMed]
10. Song, X.Q.; Zheng, Q.F.; Wang, L.; Liu, W.S. Synthesis and luminescence properties of lanthanide complexes with a new tripodal ligand featuring N-thenylsalicylamide arms. *Luminescence* **2010**, *25*, 328–335. [CrossRef] [PubMed]
11. Li, X.Y.; Chen, L.; Gao, L.; Zhang, Y.; Akogun, S.F.; Dong, W.K. Syntheses, crystal structures and catalytic activities of two solvent-induced homotrinuclear Co(II) complexes with a naphthalenediol-based bis(Salamo)-type tetraoxime ligand. *RSC Adv.* **2017**, *7*, 35905–35916. [CrossRef]
12. Tao, C.H.; Ma, J.C.; Zhu, L.C.; Zhang, Y.; Dong, W.K. Heterobimetallic 3d–4f Zn(II)–Ln(III) (Ln = Sm, Eu, Tb and Dy) complexes with a N_2O_4 bisoxime chelate ligand and a simple auxiliary ligand Py: Syntheses, structures and luminescence properties. *Polyhedron* **2017**, *128*, 38–45. [CrossRef]
13. Dong, W.K.; Zhang, J.; Zhang, Y.; Li, N. Novel multinuclear transition metal(II) complexes based on an asymmetric salamo-type ligand: Syntheses, structure characterizations and fluorescent properties. *Inorg. Chim. Acta* **2016**, *444*, 95–102. [CrossRef]
14. Song, X.Q.; Liu, P.P.; Liu, Y.A.; Zhou, J.J.; Wang, X.L. Two dodecanuclear heterometallic $[Zn_6Ln_6]$ clusters constructed by a multidentate salicylamide salen-like ligand: Synthesis, structure, luminescence and magnetic properties. *Dalton Trans.* **2016**, *45*, 8154–8163. [CrossRef] [PubMed]
15. Wu, H.L.; Pan, G.L.; Wang, H.; Wang, X.L.; Bai, Y.C.; Zhang, Y.H. Study on synthesis, crystal structure, antioxidant and DNA-binding of mono-, di- and poly-nuclear lanthanides complexes with bis(*N*-salicylidene)-3-oxapentane-1,5-diamine. *J. Photochem. Photobio. B* **2014**, *135*, 33–43. [CrossRef] [PubMed]
16. Wu, H.L.; Pan, G.L.; Bai, Y.C.; Wang, H.; Kong, J.; Shi, F.; Zhang, Y.H.; Wang, X.L. Preparation, structure, DNA-binding properties, and antioxidant activities of a homodinuclear erbium(III) complex with a pentadentate Schiff base ligand. *J. Chem. Res.* **2014**, *38*, 211–217. [CrossRef]

17. Wu, H.L.; Pan, G.L.; Bai, Y.C.; Wang, H.; Kong, J.; Shi, F.R.; Zhang, Y.H.; Wang, X.L. A Schiff base bis(*N*-salicylidene)-3-oxapentane-1,5-diamine and its yttrium(III) complex: Synthesis, crystal structure, DNA-binding properties, and antioxidant activities. *J. Coord. Chem.* **2013**, *66*, 2634–2646. [CrossRef]
18. Wu, H.L.; Bai, Y.C.; Zhang, Y.H.; Pan, G.L.; Kong, J.; Shi, F.; Wang, X.L. Two lanthanide(III) complexes based on the Schiff base *N*,*N*-bis(salicylidene)-1,5-diamino-3-oxapentane: Synthesis, characterization, DNA-binding properties, and antioxidation. *Z. Anorg. Allg. Chem.* **2014**, *640*, 2062–2071. [CrossRef]
19. Chen, C.Y.; Zhang, J.W.; Zhang, Y.H.; Yang, Z.H.; Wu, H.L. Gadolinium(III) and dysprosium(III) complexes with a Schiff base bis(*N*-salicylidene)-3-oxapentane-1,5-diamine: Synthesis, characterization, antioxidation, and DNA-binding studies. *J. Coord. Chem.* **2015**, *68*, 1054–1071. [CrossRef]
20. Wu, H.L.; Wang, C.P.; Wang, F.; Peng, H.P.; Zhang, H.; Bai, Y.C. A new manganese(III) complex from bis(5-methylsalicylaldehyde)-3-oxapentane-1,5-diamine: Synthesis, characterization, antioxidant activity and luminescence. *J. Chin. Chem. Soc.* **2015**, *62*, 1028–1034. [CrossRef]
21. Wu, H.L.; Pan, G.L.; Bai, Y.C.; Wang, H.; Kong, J. Synthesis, structure, antioxidation, and DNA-bindingstudies of a binuclear ytterbium(III) complex with bis(*N*-salicylidene)-3-oxapentane-1,5-diamine. *Res. Chem. Intermed.* **2015**, *41*, 3375–3388. [CrossRef]
22. Dong, W.K.; Lan, P.F.; Zhou, W.M.; Zhang, Y. Salamo-type trinuclear and tetranuclear cobalt(II) complexes based on a new asymmetry Salamotype ligand: Syntheses, crystal structures, and fluorescence properties. *J. Coord. Chem.* **2016**, *65*, 1272–1283. [CrossRef]
23. Dong, W.K.; Ma, J.C.; Zhu, L.C.; Zhang, Y.; Li, X.L. Four new nickel(II) complexes based on an asymmetric Salamo-type ligand: Synthesis, structure, solvent effect and electrochemical property. *Inorg. Chim. Acta* **2016**, *445*, 140–148. [CrossRef]
24. Hu, J.H.; Li, J.B.; Qi, J.; Sun, Y. Selective colorimetric and "turn-on" fluorimetric detection of cyanide using an acylhydrazone sensor in aqueous media. *New J. Chem.* **2015**, *39*, 4041–4046. [CrossRef]
25. Hu, J.H.; Li, J.B.; Qi, J.; Chen, J.J. Highly selective and effective mercury (II) fluorescent sensor. *New J. Chem.* **2015**, *39*, 843–848. [CrossRef]
26. Hu, J.H.; Yan, N.P.; Chen, J.J.; Li, J.B. Synthesis of azosalicylic aldehyde of benzoyl hydrazone based sensor and it's colorimetric sensing properties for cyanide anions in aqueous solutions. *Chem. J. Chin. Univ.* **2013**, *34*, 1368–1373.
27. Li, J.B.; Hu, J.H.; Chen, J.J.; Qi, J. Cyanide detection using a benzimidazole derivative in aqueous media. *Spectrochim. Acta A* **2014**, *133*, 773–777. [CrossRef] [PubMed]
28. Hu, J.H.; Li, J.B.; Qi, J.; Sun, Y. Acylhydrazone based fluorescent chemosensor for zinc in aqueous solution with high selectivity and sensitivity. *Sens. Actuators B* **2015**, *208*, 581–587. [CrossRef]
29. Sun, Y.; Hu, J.H.; Qi, J.; Li, J.B. A highly selective colorimetric and "turn-on" fluorimetric chemosensor for detecting CN^- based on unsymmetrical azine derivatives in aqueous media. *Spectrochim. Acta A* **2016**, *167*, 101–105. [CrossRef] [PubMed]
30. Qi, J.; Hu, J.H.; Chen, J.J.; Sun, Y.; Li, J.B. Cyanide detection using azo-acylhydrazone in aqueous media with high sensitivity and selectivity. *Current Anal. Chem.* **2016**, *12*, 119–123. [CrossRef]
31. Hu, J.H.; Li, J.B.; Qi, J.; Sun, Y. Studies on the crystal structure and characterization of *N*-(4-acetylphenyl)-*N*′-(2-nitrobenzoyl)-thiourea. *Phosphorus Sulfur Silicon Relat. Elem.* **2016**, *191*, 984–987. [CrossRef]
32. Hu, J.H.; Sun, Y.; Qi, J.; Li, Q.; Wei, T.B. A new unsymmetrical azine derivative based on coumarin group as dual-modal sensor for CN- and fluorescent "OFF–ON" for Zn^{2+}. *Spectrochim. Acta A* **2017**, *175*, 125–133. [CrossRef] [PubMed]
33. Sun, Y.X.; Zhang, S.T.; Ren, Z.L.; Dong, X.Y.; Wang, L. Synthesis, characterization, and crystal structure of a new supramolecular Cd^{II} complex with halogen-substituted salen-type bisoxime. *Synth. React. Inorg. Met.-Org. Nano-Met. Chem.* **2013**, *43*, 995–1000. [CrossRef]
34. Zhao, L.; Dang, X.T.; Chen, Q.; Zhao, J.X.; Wang, L. Synthesis, crystal structure and spectral properties of a 2D supramolecular copper(II) complex with 1-(4-{[(*E*)-3-ethoxyl-2-hydroxybenzylidene]amino}phenyl)ethanone oxime. *Synth. React. Inorg. Met.-Org. Nano-Met. Chem.* **2013**, *43*, 1241–1246. [CrossRef]
35. Dong, X.Y.; Li, X.Y.; Liu, L.Z.; Zhang, H.; Ding, Y.J.; Dong, W.K. Tri- and hexanuclear heterometallic Ni(II)–M(II) (M = Ca, Sr and Ba) bis(salamo)-type complexes: Synthesis, structure and fluorescence properties. *RSC Adv.* **2017**, *7*, 48394–48403. [CrossRef]
36. Darensbourg, D.J. Making plastics from carbon dioxide: Salen metal complexes as catalysts for the production of polycarbonates from epoxides and CO_2. *Chem. Rev.* **2007**, *107*, 2388–2410. [CrossRef] [PubMed]

37. Li, L.H.; Dong, W.K.; Zhang, Y.; Akogun, S.F.; Xu, L. Syntheses, structures and catecholase activities of homo-and hetero-trinuclear cobalt(II) complexes constructed from an acyclic naphthalenediol-based bis(salamo)-type ligand. *Appl. Organomet. Chem.* **2017**, *31*, e3818. [CrossRef]
38. Chai, L.Q.; Huang, J.J.; Zhang, H.S.; Zhang, Y.L.; Zhang, J.Y.; Li, Y.X. An unexpected cobalt(III) complex containing a Schiff base ligand: Synthesis, crystal structure, spectroscopic behavior, electrochemical property and SOD-like activity. *Spectrochim. Acta A* **2014**, *131*, 526–533. [CrossRef] [PubMed]
39. Chai, L.Q.; Tang, L.J.; Chen, L.C.; Huang, J.J. Structural, spectral, electrochemical and DFT studies of two mononuclear manganese(II) and zinc(II) complexes. *Polyhedron* **2017**, *122*, 228–240. [CrossRef]
40. Chai, L.Q.; Zhang, K.Y.; Tang, L.J.; Zhang, J.Y.; Zhang, H.S. Two mono- and dinuclear Ni(II) complexes constructed from quinazoline-type ligands: Synthesis, X-ray structures, spectroscopic, electrochemical, thermal, and antimicrobial studies. *Polyhedron* **2017**, *130*, 100–107. [CrossRef]
41. Li, G.; Hao, J.; Liu, L.Z.; Zhou, W.M.; Dong, W.K. Syntheses, crystal structures and thermal behaviors of two supramolecular salamo-type cobalt(II) and zinc(II) complexes. *Crystals* **2017**, *7*, 217. [CrossRef]
42. Chai, L.Q.; Mao, K.H.; Zhang, J.Y.; Zhang, K.Y.; Zhang, H.S. Synthesis, X-ray crystal structure, spectroscopic, electrochemical and antimicrobial studies of a new dinuclear cobalt(III) complex. *Inorg. Chim. Acta* **2017**, *457*, 34–40. [CrossRef]
43. Akine, S.; Taniguchi, T.; Nabeshima, T. Synthesis and characterization of novel ligands 1,2-Bis (salicylideneaminooxy)ethanes. *Chem. Lett.* **2001**, *30*, 682–683. [CrossRef]
44. Dong, Y.J.; Dong, X.Y.; Dong, W.K.; Zhang, Y.; Zhang, L.S. Three asymmetric Salamo-type copper(II) and cobalt(II) complexes: Syntheses, structures, fluorescent properties. *Polyhedron* **2017**, *123*, 305–315. [CrossRef]
45. Zhao, L.; Wang, L.; Sun, Y.X.; Dong, W.K.; Tang, X.L.; Gao, X.H. A supramolecular copper(II) complex bearing salen-type bisoxime ligand: Synthesis, structural characterization, and thermal property. *Synth. React. Inorg. Met.-Org. Nano-Met. Chem.* **2012**, *42*, 1303–1308. [CrossRef]
46. Akine, S.; Taniguchi, T.; Nabeshima, T. Acyclic bis(N_2O_2 chelate) ligand for trinuclear d-block homo- and heterometal complexes. *Inorg. Chem.* **2008**, *47*, 3255–3264. [CrossRef] [PubMed]
47. Zheng, S.S.; Dong, W.K.; Zhang, Y.; Chen, L.; Ding, Y.J. Four Salamo-type 3d–4f hetero-bimetallic [$Zn^{II}Ln^{III}$] complexes: Syntheses, crystal structures, and luminescent and magnetic properties. *New J. Chem.* **2017**, *41*, 4966–4973. [CrossRef]
48. Dong, Y.J.; Li, X.L.; Zhang, Y.; Dong, W.K. A highly selective visual and fluorescent sensor for Pb^{2+} and Zn^{2+} and crystal structure of Cu^{2+} complex based-on a novel single-armed Salamo-type bisoxime. *Supramol. Chem.* **2017**, *29*, 518–527. [CrossRef]
49. Dong, W.K.; Ma, J.C.; Zhu, L.C.; Zhang, Y. Nine self–assembled nickel(II)-lanthanide(III) heterometallic complexes constructed from a Salamo–type bisoxime and bearing *N*- or *O*-donor auxiliary ligand: Syntheses, structures and magnetic properties. *New J. Chem.* **2016**, *40*, 6998–7010. [CrossRef]
50. Song, X.Q.; Wang, L.; Zheng, Q.F.; Liu, W.S. Synthesis, crystal structure and luminescence properties of lanthanide complexes with a new semirigid bridging furfurylsalicylamide ligand. *Inorg. Chim. Acta* **2013**, *391*, 171–178. [CrossRef]
51. Chai, L.Q.; Liu, G.; Zhang, J.Y.; Huang, J.J.; Tong, J.F. Synthesis, crystal structure, fluorescence, electrochemical property, and SOD-like activity of an unexpected nickel(II) complex with a quinazoline-type ligand. *J. Coord. Chem.* **2013**, *66*, 3926–3938. [CrossRef]
52. Ma, J.C.; Dong, X.Y.; Dong, W.K.; Zhang, Y.; Zhu, L.C.; Zhang, J.T. An unexpected dinuclear Cu(II) complex with a bis(Salamo) chelating ligand: Synthesis, crystal structure, and photophysical properties. *J. Coord. Chem.* **2016**, *69*, 149–159. [CrossRef]
53. Hao, J.; Liu, L.Z.; Dong, W.K.; Zhang, J.; Zhang, Y. Three multinuclear Co(II), Zn(II) and Cd(II) complexes based on a single-armed salamo-type bisoxime: Syntheses, structural characterizations and fluorescent properties. *J. Coord. Chem.* **2017**, *70*, 1936–1952. [CrossRef]
54. Liu, P.P.; Sheng, L.; Song, X.Q.; Xu, W.Y.; Liu, Y.A. Synthesis, structure and magnetic properties of a new one dimensional manganese coordination polymer constructed by a new asymmetrical ligand. *Inorg. Chim. Acta* **2015**, *434*, 252–257. [CrossRef]
55. Griffiths, K.; Gallop, C.W.D.; Abdul-Sada, A.; Vargas, A.; Navarro, O.; Kostakis, G.E. Heteronuclear 3d/Dy^{III} coordination clusters as catalysts in a domino reaction. *Chem. Eur. J.* **2015**, *21*, 6358–6361. [CrossRef] [PubMed]

56. Griffiths, K.; Kumar, P.; Akien, G.R.; Chilton, N.F.; Abdul-Sada, A.; Tizzard, G.J.; Coles, S.J.; Kostakis, G.E. Tetranuclear Zn/4f coordination clusters as highly efficient catalysts for Friedel-Crafts alkylation. *Chem. Commun.* **2016**, *52*, 7866–7869. [CrossRef] [PubMed]
57. Kumar, P.; Griffiths, K.; Lymperopoulou, S.; Kostakis, G.E. Tetranuclear Zn_2Ln_2 coordination clusters as catalysts in the petasis borono-mannich multicomponent reaction. *RSC Adv.* **2016**, *6*, 79180–79184. [CrossRef]
58. Griffiths, K.; Kumar, P.; Mattock, J.D.; Abdul-Sada, A.; Pitak, M.B.; Coles, S.J.; Navarro, O.; Vargas, A.; Kostakis, G.E. Efficient $Ni^{II}{}_2Ln^{III}{}_2$ electrocyclization catalysts for the synthesis of trans-4,5-diaminocyclopent-2-enones from 2-furaldehyde and primary or secondary amines. *Inorg. Chem.* **2016**, *55*, 6988–6994. [CrossRef] [PubMed]
59. Kumar, P.; Lymperopoulou, S.; Griffiths, K.; Sampani, S.I.; Kostakis, G.E. Highly efficient tetranuclear $Zn^{II}{}_2Ln^{III}{}_2$ catalysts for the friedel-crafts alkylation of indoles and nitrostyrenes. *Catalysts* **2016**, *6*, 140. [CrossRef]
60. Griffiths, K.; Tsipis, A.C.; Kumar, P.; Townrow, O.P.E.; Abdul-Sada, A.; Akien, G.R.; Baldansuren, A.; Spivey, A.C.; Kostakis, G.E. 3d/4f coordination clusters as cooperative catalysts for highly diastereoselective michael addition reactions. *Inorg. Chem.* **2017**, *56*, 9563–9573. [CrossRef] [PubMed]
61. Sampani, S.I.; Aubert, S.; Cattoen, M.; Griffiths, K.; Abdul-Sada, A.; Akien, G.R.; Tizzard, G.J.; Coles, S.J.; Arseniyadis, S.; Kostakis, G.E. Dinucleating Schiff base ligand in Zn/4f coordination chemistry: Synthetic challenges and catalytic activity evaluation. *Dalton Trans.* **2018**, *47*, 4486–4493. [CrossRef] [PubMed]
62. Wang, L.; Hao, J.; Zhai, L.X.; Zhang, Y.; Dong, W.K. Synthesis, crystal structure, luminescence, electrochemical and antimicrobial properties of bis(salamo)-based Co(II) complex. *Crystals* **2017**, *7*, 277. [CrossRef]
63. Sheldrick, G.M. *SHELXL-2016, Program for Crystal Structure Refinement*; University of Göttingen: Göttingen, Germany, 1997.
64. Gao, L.; Wang, F.; Zhao, Q.; Zhang, Y.; Dong, W.K. Mononuclear Zn(II) and trinuclear Ni(II) complexes derived from a coumarin-containing N_2O_2 ligand: Syntheses, crystal structures and fluorescence properties. *Polyhedron* **2018**, *139*, 7–16. [CrossRef]
65. Wang, P.; Zhao, L. An infinite 2D supramolecular cobalt(II) complex based on an asymmetric Salamo-type ligand: Synthesis, crystal structure, and spectral properties. *Synth. React. Inorg. Met.-Org. Nano-Met. Chem.* **2016**, *46*, 1095–1101. [CrossRef]
66. Dong, Y.J.; Ma, J.C.; Zhu, L.C.; Dong, W.K.; Zhang, Y. Four 3d–4f heteromultinuclear zinc(II)–lanthanide(III) complexes constructed from a distinct hexadentate N_2O_2-type ligand: Syntheses, structures and photophysical properties. *J. Coord. Chem.* **2017**, *70*, 103–115. [CrossRef]
67. Dong, W.K.; Zhang, F.; Li, N.; Xu, L.; Zhang, Y.; Zhang, J.; Zhu, L.C. Trinuclear cobalt(II) and zinc(II) salamo–type complexes: Syntheses, crystal structures, and fluorescent properties. *Z. Anorg. Allg. Chem.* **2016**, *642*, 532–538. [CrossRef]
68. Sun, Y.X.; Zhao, Y.Y.; Li, C.Y.; Yu, B.; Guo, J.Q.; Li, J. Supramolecular cobalt(II) and copper(II) complexes with Schiff base ligand: Syntheses, characterizations and crystal structures. *Chin. J. Inorg. Chem.* **2016**, *32*, 913–920.
69. Dong, X.Y.; Sun, Y.X.; Wang, L.; Li, L. Synthesis and structure of a penta- and hexa-coordinated tri-nuclear cobalt(II) complex. *J. Chem. Res.* **2012**, *36*, 387–390. [CrossRef]
70. Dong, X.Y.; Gao, L.; Wang, F.; Zhang, Y.; Dong, W.K. Tri- and mono-nuclear zinc(II) complexes based on half- and mono-salamo chelating ligands. *Crystals* **2017**, *7*, 267. [CrossRef]
71. Chen, L.; Dong, W.K.; Zhang, H.; Zhang, Y.; Sun, Y.X. Structural variation and luminescence properties of tri- and dinuclear Cu^{II} and Zn^{II} complexes constructed from a naphthalenediol-based bis(Salamo)-type ligand. *Cryst. Growth Des.* **2017**, *17*, 3636–3648. [CrossRef]
72. Hao, J.; Li, L.L.; Zhang, J.T.; Akogun, S.F.; Wang, L.; Dong, W.K. Four homo- and hetero-bismetallic 3d/3d-2s complexes constructed from a naphthalenediol-based acyclic bis(salamo)-type tetraoxime ligand. *Polyhedron* **2017**, *134*, 1–10. [CrossRef]
73. Dong, X.Y.; Akogun, S.F.; Zhou, W.M.; Dong, W.K. Tetranuclear Zn(II) complex based on an asymmetrical salamo-type chelating ligand: Synthesis, structural characterization, and fluorescence property. *J. Chin. Chem. Soc.* **2017**, *64*, 412–419. [CrossRef]
74. Xu, L.; Zhu, L.C.; Ma, J.C.; Zhang, Y.; Zhang, J.; Dong, W.K. Syntheses, structures and spectral properties of mononuclear Cu^{II} and dimeric Zn^{II} complexes based on an asymmetric Salamo-type N_2O_2 ligand. *Z. Anorg. Allg. Chem.* **2015**, *641*, 2520–2524. [CrossRef]

75. Dong, W.K.; Zheng, S.S.; Zhang, J.T.; Zhang, Y.; Sun, Y.X. Luminescent properties of heterotrinuclear 3d–4f complexes constructed from a naphthalenediol-based acyclic bis(salamo)-type ligand. *Spectrochim. Acta A* **2017**, *184*, 141–150. [CrossRef] [PubMed]
76. Wang, P.; Zhao, L. Synthesis, structure and spectroscopic properties of the trinuclear cobalt(II) and nickel(II) complexes based on 2-hydroxynaphthaldehyde and bis(aminooxy)alkane. *Spectrochim. Acta Part A* **2015**, *135*, 342–350. [CrossRef] [PubMed]
77. Sun, Y.X.; Wang, L.; Dong, X.Y.; Ren, Z.L.; Meng, W.S. Synthesis, characterization, and crystal structure of a supramolecular Co^{II} complex containing Salen-type bisoxime. *Synth. React. Inorg. Met.-Org. Nano-Met. Chem.* **2013**, *43*, 599–603. [CrossRef]
78. Dong, W.K.; Ma, J.C.; Zhu, L.C.; Zhang, Y. Self-assembled zinc(II)-lanthanide(III) heteromultinuclear complexes constructed from 3-MeOsalamo ligand: Syntheses, structures and luminescent properties. *Cryst. Growth Des.* **2016**, *16*, 6903–6914. [CrossRef]